Q-burst Geolocation and Characterization using the HeartMath Six-station ELF Network

Anirban Guha[1*], Paul Nicholson[2], Earle Williams[3], Yakun Liu[3], Qianqian Wang[4], Mike Atkinson[5] and Rollin McCraty[5]

[1]Department of Physics, Tripura University, India

[2]Abelian Computing Ltd., United Kingdom

[3]Civil and Environmental Engineering, Massachusetts Institute of Technology, USA

[4]Institute of Urban Meteorology, China Meteorological Administration, China

[5]Heartmath Institute, USA

*Presenting author email: anirbanguha@tripurauniv.ac.in

त्रिपुरा विश्वविद्यालय
(केंद्रीय विश्वविद्यालय)
TRIPURA UNIVERSITY
(A Central University)

HeartMath Institute
A Nonprofit Organization

北京城市气象研究院
Institute of Urban Meteorology,CMA,Beijing

Introduction (What are Q-Bursts?)

Objective: To identify, locate, and characterize powerful ELF transients ("Q-bursts") from lightning, 'Quiet' in VLF (Ogawa type, short impulse) and the bell-ringers (long continuing current).

Definition in this Study: An ELF transient significantly larger than the background, detected by a majority of a six-station network.

- Operational Definition: Detected when any station sees an amplitude >12σ above background, and at least four others see it >6σ.
- Significance: These events are associated with the most powerful lightning strokes, often with significant continuing currents.

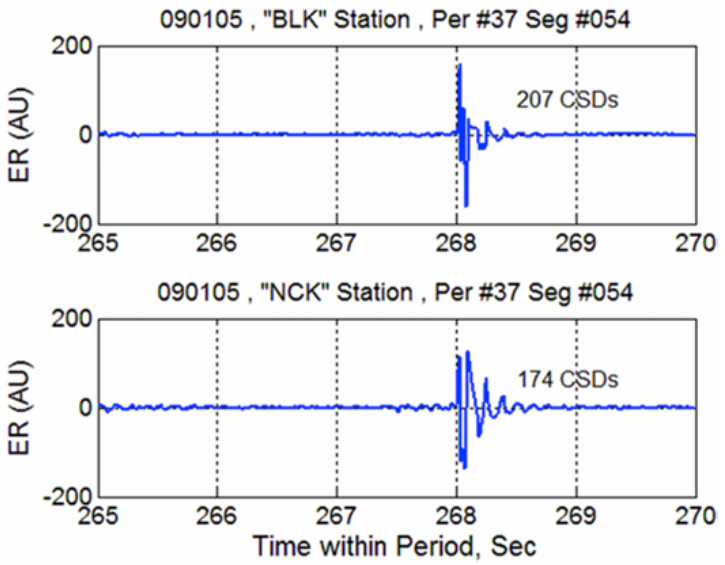

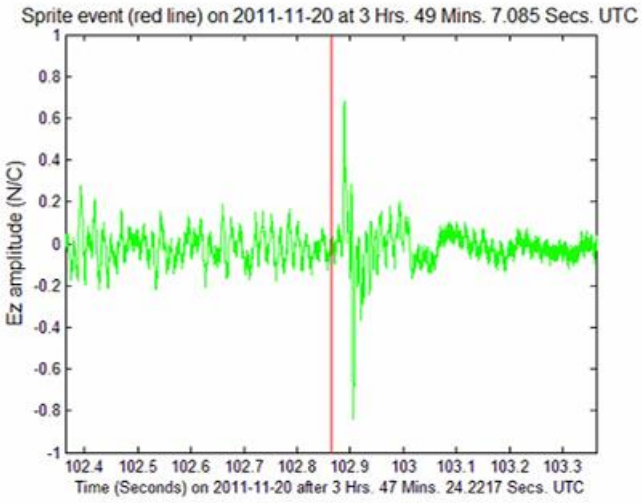

Guha et. al 2017, JASTP

Journal of Atmospheric and Solar-Terrestrial Physics 165-166 (2017) 25–37

Contents lists available at ScienceDirect

Journal of Atmospheric and Solar-Terrestrial Physics

journal homepage: www.elsevier.com/locate/jastp

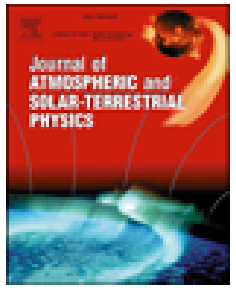

Aliasing of the Schumann resonance background signal by sprite-associated Q-bursts

Anirban Guha [a,b,*], Earle Williams [b], Robert Boldi [c], Gabriella Sátori [d], Tamás Nagy [d], József Bór [d], Joan Montanyà [e], Pascal Ortega [f]

[a] Department of Physics, Tripura University, Tripura, India
[b] Parsons Laboratory, Massachusetts Institute of Technology, Cambridge, MA, USA
[c] College of Natural and Health Sciences, Zayed University, Dubai, United Arab Emirates
[d] Research Centre for Astronomy and Earth Sciences, GGI, Hungarian Academy of Sciences, Sopron, Hungary
[e] Electrical Engineering Department, Polytechnic University of Catalonia, Barcelona, Spain
[f] Laboratory GEPASUD, University of French Polynesia, Tahiti, French Polynesia

Scientific Interests

- Global spatio-temporal characterization of TLE producing Q-bursts, as observation of TLEs are possible only during nighttime.
- Continuous observation of Q-bursts to infer deeper understanding about their occurrence, climatology and charge transfer to the upper atmosphere.
- Global spatio-temporal variation of Q-bursts could differ from the global 'ordinary' lightning climatology, relating to the late and mature stage of development of thunderstorms.
- The evolution of Q-bursts in MCCs and MCSs.
- Chimney to chimney variability, diurnal and seasonal variability of global Q-bursts.

The Sensor Network & Data Pipeline

- **Network:** Six 2-axis ELF magnetometer stations (Heartmath Institute network).
- **Data Period:** 489 days (April 2017 – June 2024).

Preprocessing Steps:

- Original sampling at 130 Hz. Resample to 520 Hz, UT-synchronized. Filter (1 Hz high-pass, 63 Hz low-pass, notch filters).
- Combine into 12 channels (EW/NS for 6 sites).
  [Hphi = sqrt (Hx^2+Hy^2), all thresholds apply to Hphi]
- Convert to 6 horizontal magnitude channels for detection.

https://www.heartmath.org/gci/gcms/

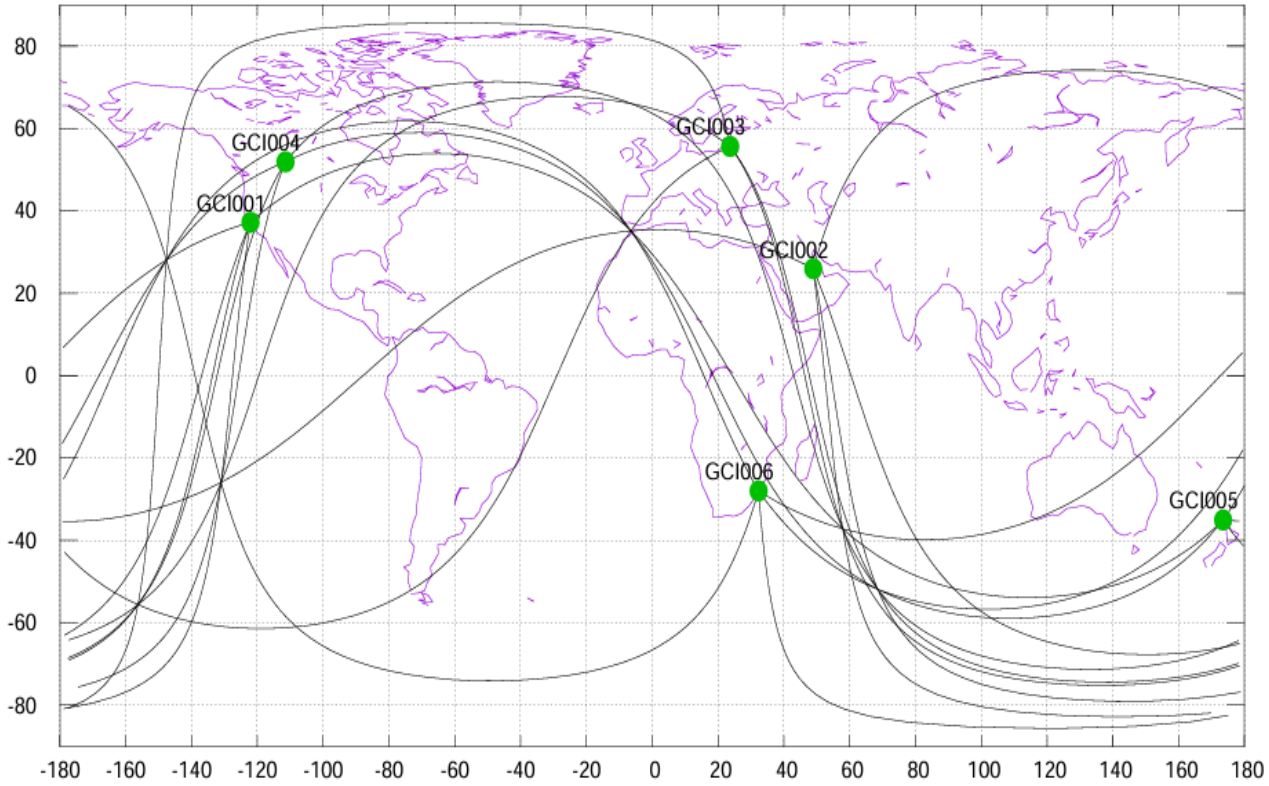

GCI001 = Boulder Creek, CA USA (BOU)
GCI002 = Hofuf, Saudi Arabia (HOF)
GCI003 = Baisogala, Lithuania (BAI)
GCI004 = Alberta, Canada (ALB)
GCI005 = Northland, New Zealand (NOR)
GCI006 = Hluhluwe, South Africa (HLU)

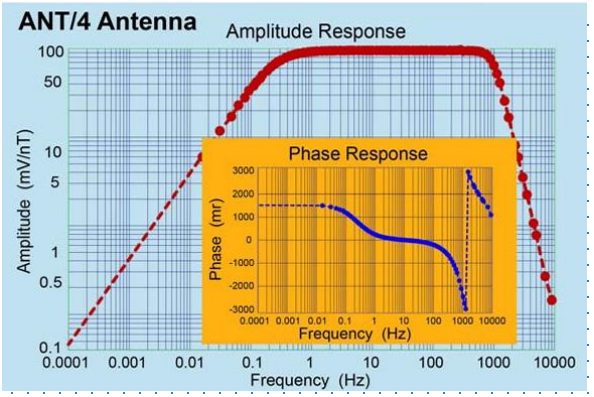

Pulse Detection Algorithm

Method: A "scanning window" mimics manual analysis of a 6-channel chart.

- Preamble (60 ms): Searches for quiet background.
- Measurement (100 ms): Looks for pulses above threshold.

Key Features:

- Detects earliest pulse per channel.
- Uses dynamic thresholds (6σ to 60σ) to capture weak and strong events.
- Incorporates a "quiet time" before detection to avoid ringing.

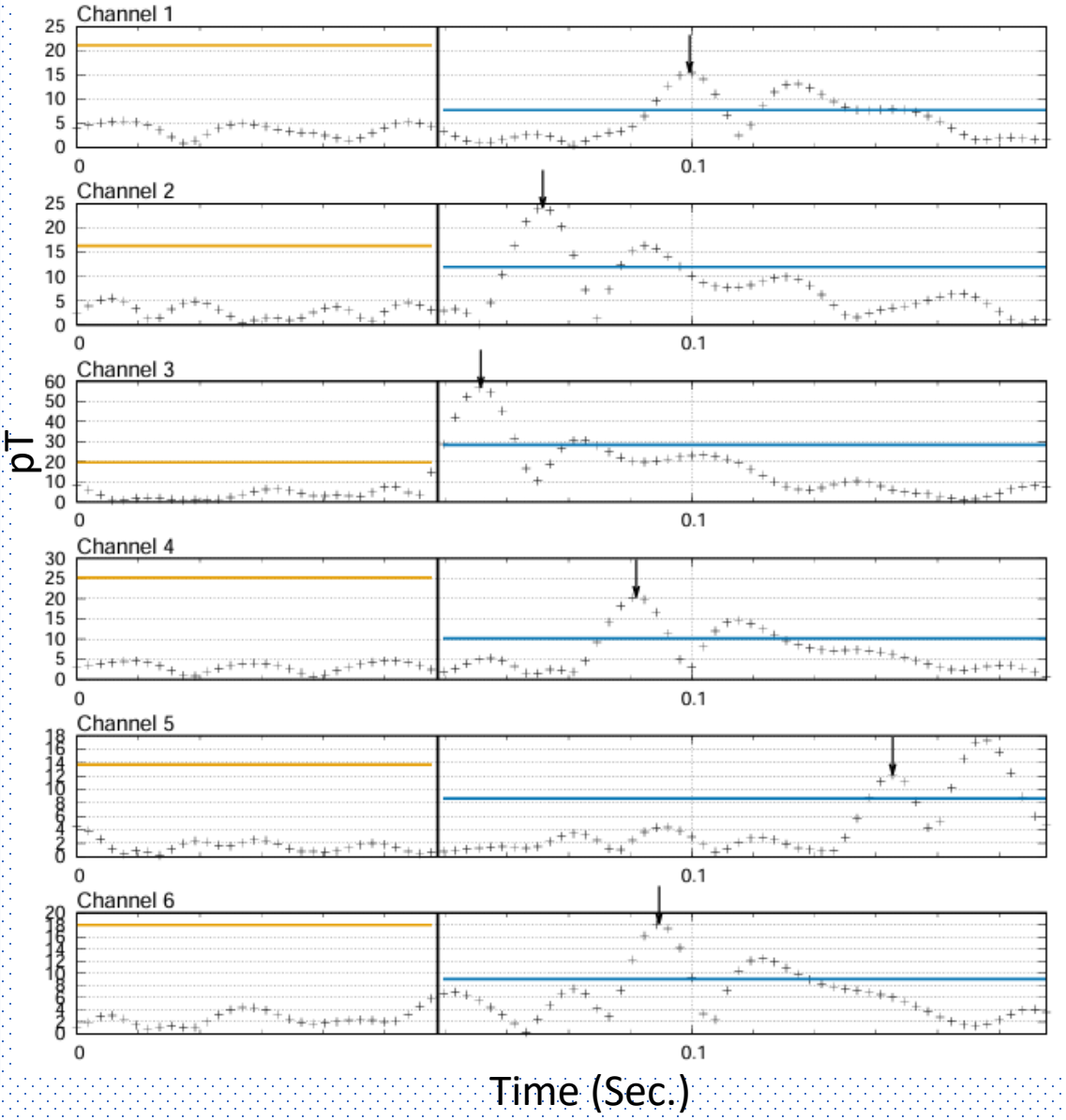

Locating the Source: Triangulation & Trilateration

- **Method:** Combines time of arrival (trilateration) and azimuth (triangulation)
- **Key Challenge:** Propagation velocity in the Earth-ionosphere waveguide is not constant.
- **Solution Approach:** Use a "velocity factor" (Vf) to model speed as a fraction of the speed of light (c).
- **Cost Function:** Uses a robust metric to reject "rogue" pulse timings from noise or other strokes.

The Optimal Velocity Factor

Experiment: Processed 19 days of data with different fixed velocity factors (Vf = 0.74 to 0.87 c).

Evaluation Metrics:

- Number of solutions.
- Mean residual cost.
- Standard deviation of timing errors.

Result: The optimum constant velocity factor is ~0.80c - 0.81c.

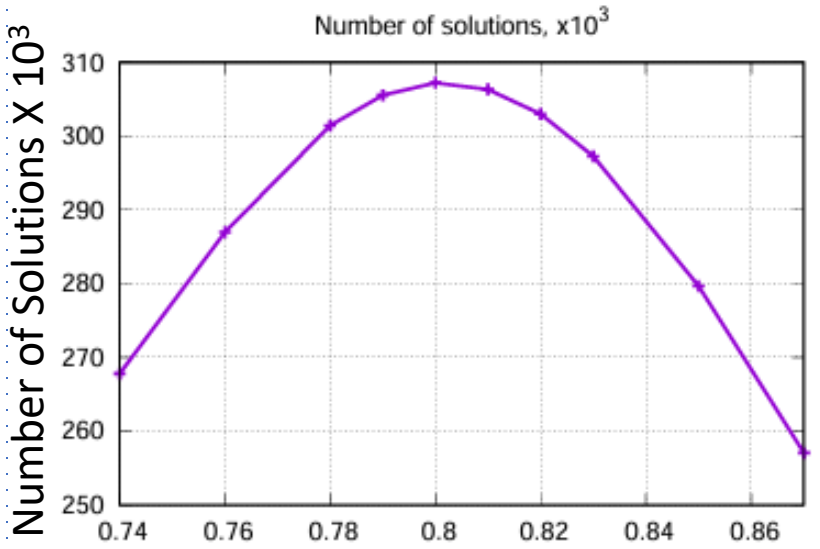

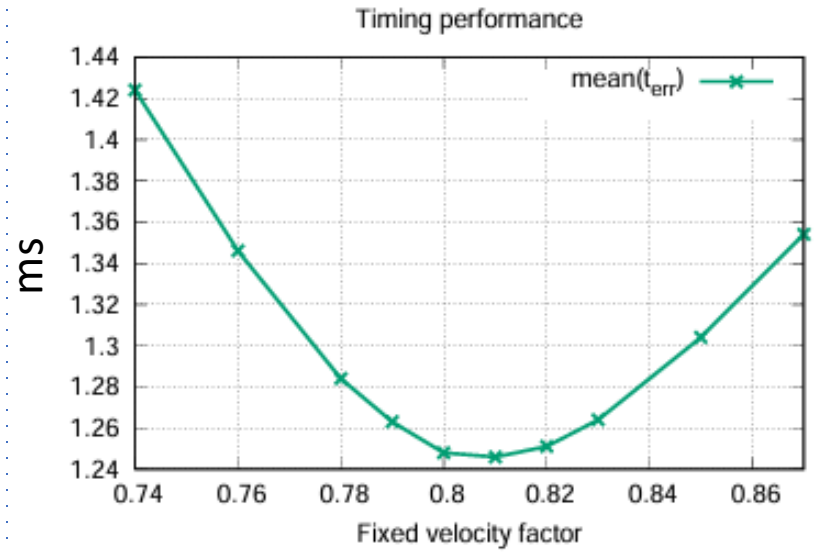

Validating with WWLLN (Ground Truth)

Goal: Compare our Q-burst solutions with strokes from the World Wide Lightning Location Network (WWLLN).

Matching Criteria:

- Time difference: -5 ms < Δt < +9 ms
- Distance difference: < 1000 km
- No other WWLLN solution within the bounding box defined by the time and distance limits.

Outcome with Vf = 0.80c: ~46% of Q-bursts matched WWLLN strokes with a mean distance error of 550 km.

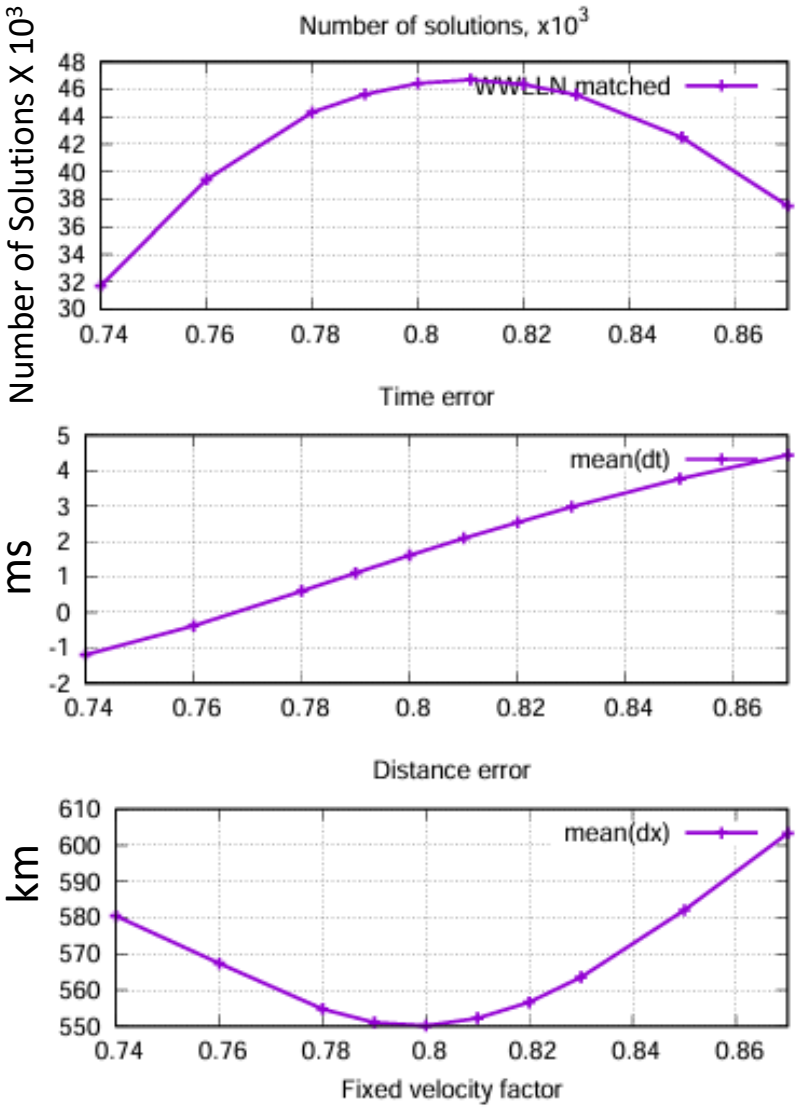

Q-burst Polarity

- **Technique:** Using the known location, we can synthesize a virtual coil oriented towards the source to get the maximum signal (Bϕ). [Ampere's law]

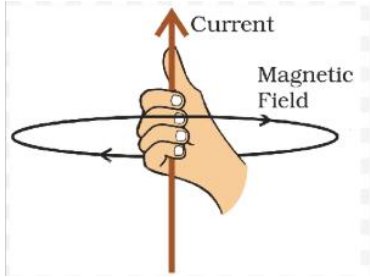

- We determine that coil wiring is such that positive lightning to the south-east produces positive going signals in both coils, thus the oriented signal is given by $H_\theta = H_{ns}\sin(\theta) - H_{ew}\cos(\theta)$

  where θ is the azimuth of the Q-burst as seen from the receiver site.

- **Polarity Insight:** The oriented waveform reveals the source's polarity.

- The majority of the strongest Q-bursts are positive.

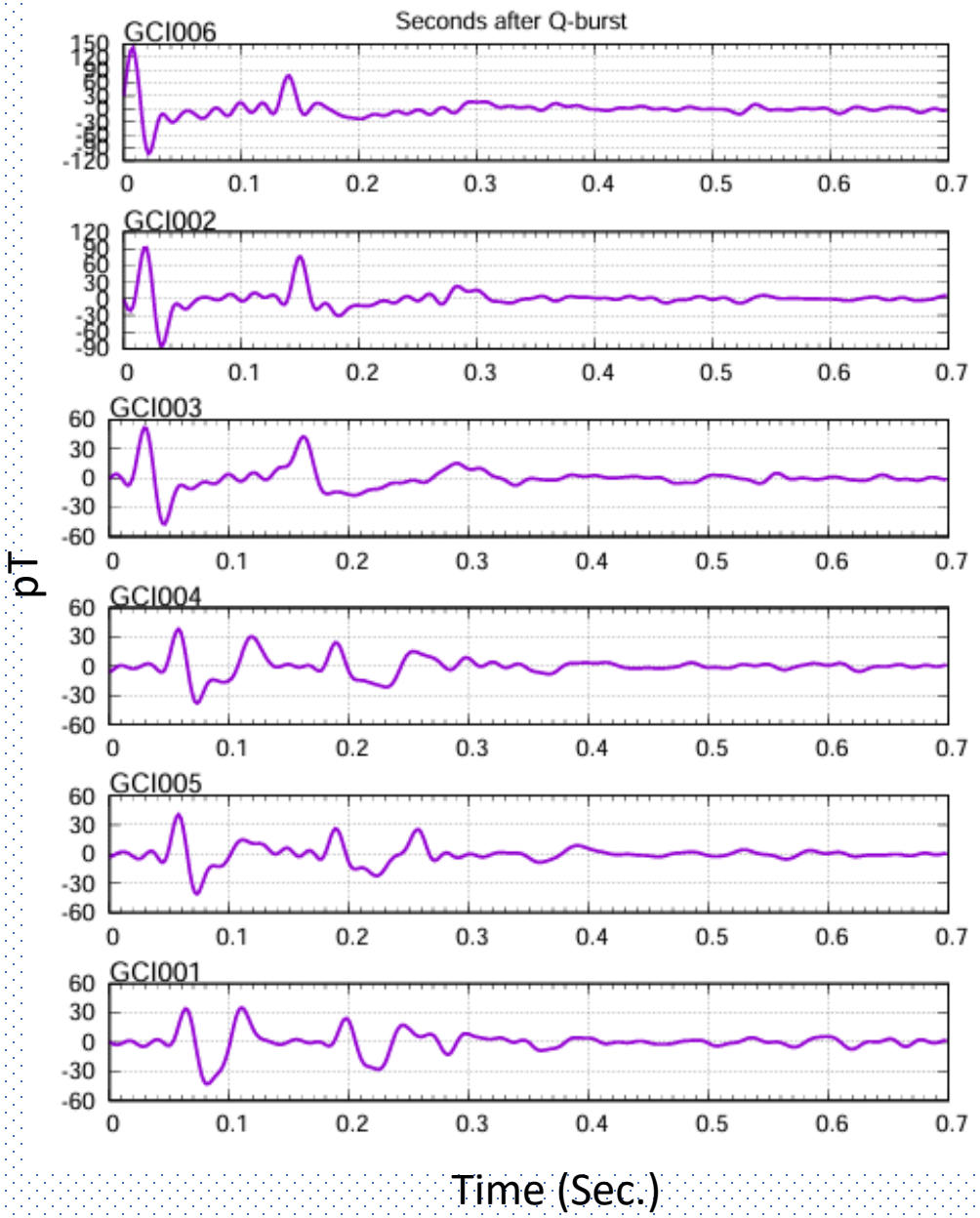

Spectra of Q-Bursts

- **Analysis:** Compute the spectra of the oriented signals.
- **Observation:** The Schumann resonances (global EM resonances) are prominently excited.
- **Note:** The lowest resonance frequency appears lower (~6.3 Hz) on the closest receiver, a notable observation.

Spectra of the oriented signal at each receiver showing the relative RMS amplitude in 0.1 Hz bins, plotted in order(left to right, top to bottom) of increasing distance from the Q-burst.

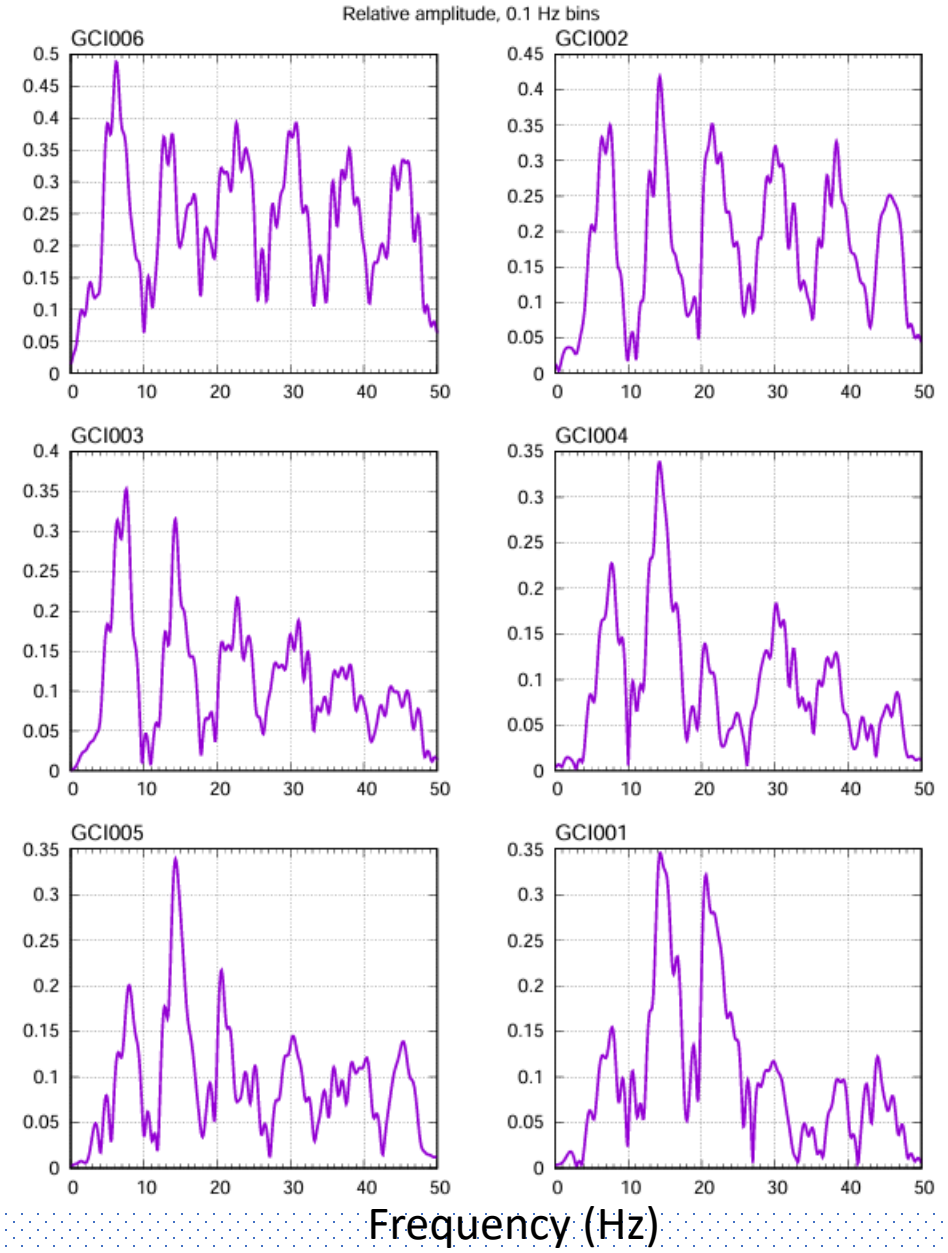

Building a Better Model: Path Statistics

Limitation of Constant Vf: Propagation is anisotropic (depends on direction and solar illumination).

Data Source: Used 836k paths from 143k WWLLN-matched Q-bursts.

Key Parameters per Path:

- Propagation time (WWLLN time to pulse peak).
- Path length.
- Illumination Factor: % of path under sunlight.
- Receiver Azimuth: Direction of propagation.

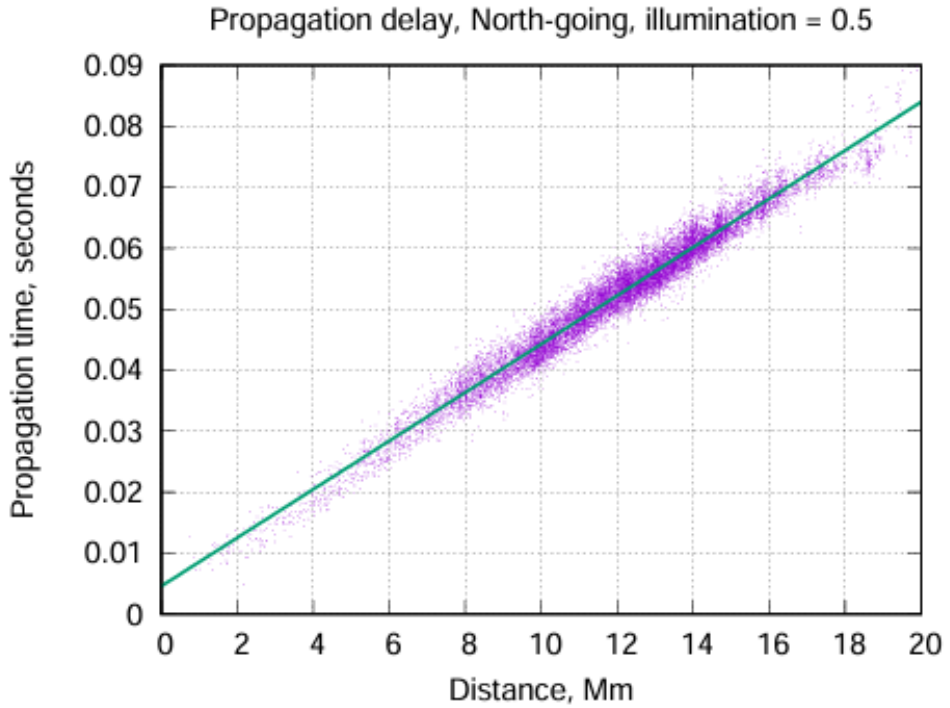

The 2D (Azimuth & Solar Illumination) Propagation Model

Model Development: Create a lookup table with 21 illumination bands x 4 cardinal azimuths.

Result: Each path segment is assigned a specific velocity factor and a zero-range offset.

Performance Improvement:

- WWLLN Match Rate increased to 67% from 46%.
- Mean Location Error decreased to 417 km from 550 km

B_h (nT)	-90/-60	-60/-40	-40/-20	-20/0	0/+20	+20/+40	+40/+60	+60/+90
-36000	0.941	0.915	0.904	0.870	0.778	0.789	0.782	0.797
-32000	0.909	0.905	0.897	0.872	0.800	0.802	0.808	0.810
-28000	0.899	0.904	0.900	0.870	0.794	0.789	0.790	0.800
-24000	0.908	0.913	0.899	0.856	0.794	0.786	0.785	0.804
-20000	0.896	0.893	0.896	0.850	0.790	0.773	0.782	0.794
-16000	0.899	0.900	0.893	0.834	0.779	0.760	0.771	0.803
-12000	0.880	0.895	0.890	0.831	0.773	0.771	0.775	0.786
-8000	0.894	0.885	0.880	0.838	0.775	0.766	0.782	0.800
-4000	0.884	0.878	0.875	0.839	0.773	0.765	0.774	0.792
0	0.879	0.868	0.866	0.833	0.777	0.764	0.772	0.800
+4000	0.898	0.886	0.876	0.846	0.782	0.758	0.774	0.796
+8000	0.918	0.901	0.897	0.842	0.791	0.771	0.776	0.800
+12000	0.898	0.891	0.882	0.837	0.787	0.771	0.772	0.790
+16000	0.899	0.893	0.885	0.840	0.782	0.775	0.780	0.797
+20000	0.928	0.927	0.918	0.877	0.797	0.796	0.801	0.804
+24000	0.881	0.894	0.913	0.864	0.781	0.783	0.805	0.801
+28000	0.911	0.910	0.912	0.864	0.792	0.773	0.792	0.807
+32000	0.941	0.923	0.927	0.875	0.805	0.800	0.795	0.806
+36000	0.970	0.954	0.960	0.900	0.824	0.815	0.823	0.836

Final Data Run & Statistics

Scope: Processed the full 489-day dataset (11,601 hours) from 2017-04-08 to 2024-06-10 using the 2D model.

Outcome: Identified 4,543,886 Q-bursts.

Final Validation:

- Matched 67.1% to WWLLN strokes.
- Mean location error: 417 km.
- RMS timing error: 2.2 ms.

Global Rate: ~1 Q-burst every 9.2 seconds.

Deriving Source Properties: Charge Moment

Goal: Reconstruct the source current moment (I(t)·ds) from the received Bϕ(t).

Process:

- Remove the transfer function of the Earth-ionosphere cavity (uniform model h= 70 km). [Huang et al., 1999]
- Remove the system transfer function (magnetometer + filters).
- Average spectra from multiple receivers to get source spectrum.
- Transform back to time domain to get source current moment.

Outputs:

Integrate the source current moment waveform from (t = 0) and record the integration value at three points: after the first 20mS (**icm1**), at the first zero crossing (**icm2**), and after 0.2 seconds (**icm3**). Also record the time taken to reach the first zero crossing of the current (**ttz**).

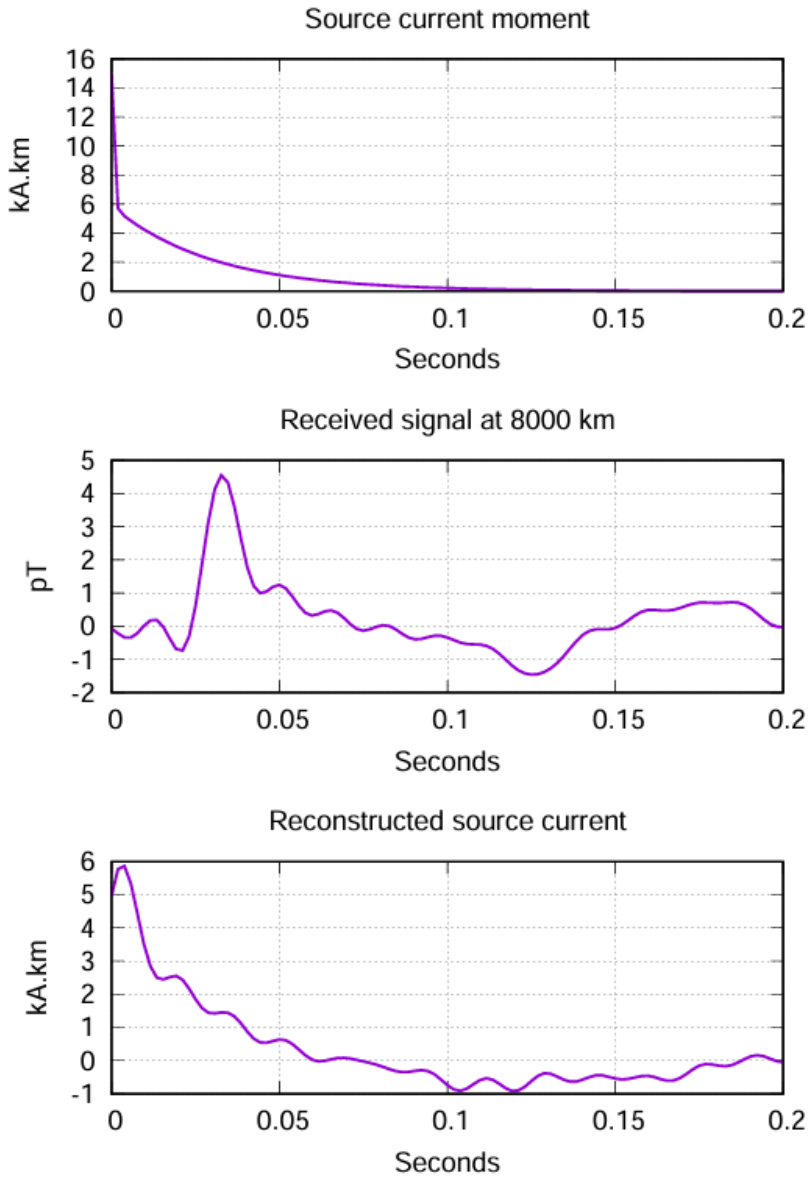

Global Geographic Distribution Total Events

- **Mapping:** 1° x 1° density maps of Q-burst count and charge moment.
- **Key Finding 1:** Positive and negative Q-bursts have distinct global distributions.
- **Key Finding 2:** Peaks in positive events at ~-28° and +34° latitude, aligning with regions of +CG lightning.
- **Key Finding 3:** The highest overall event rates are near the equator, dominated by Africa.

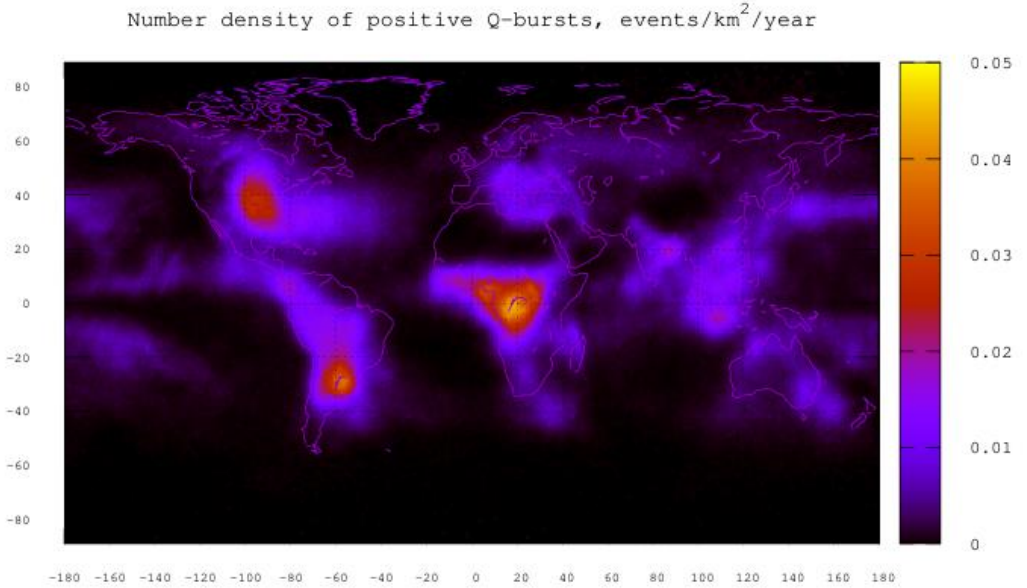

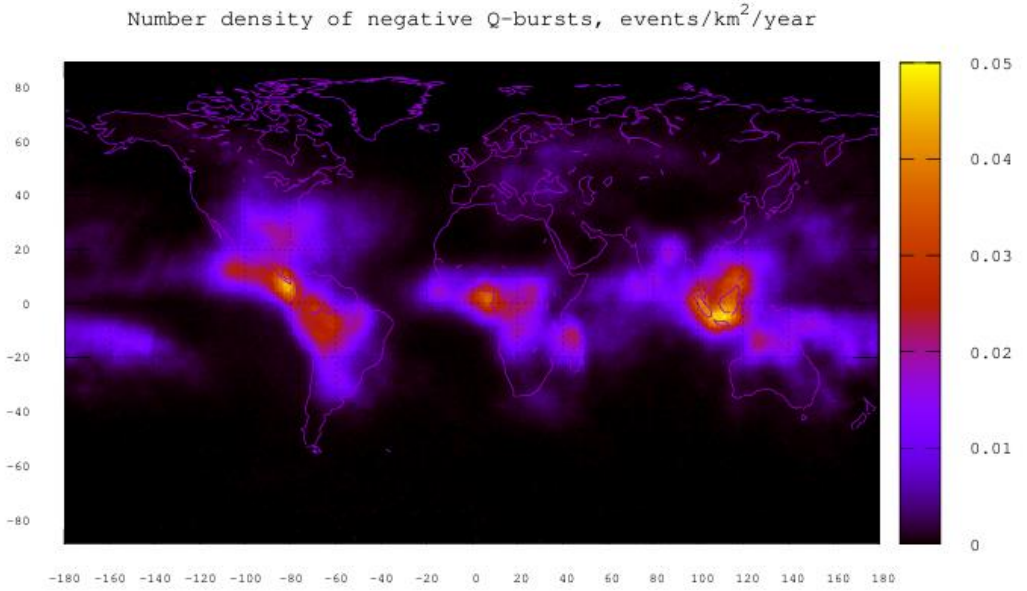

Global UT Diurnal Variation of Total Events

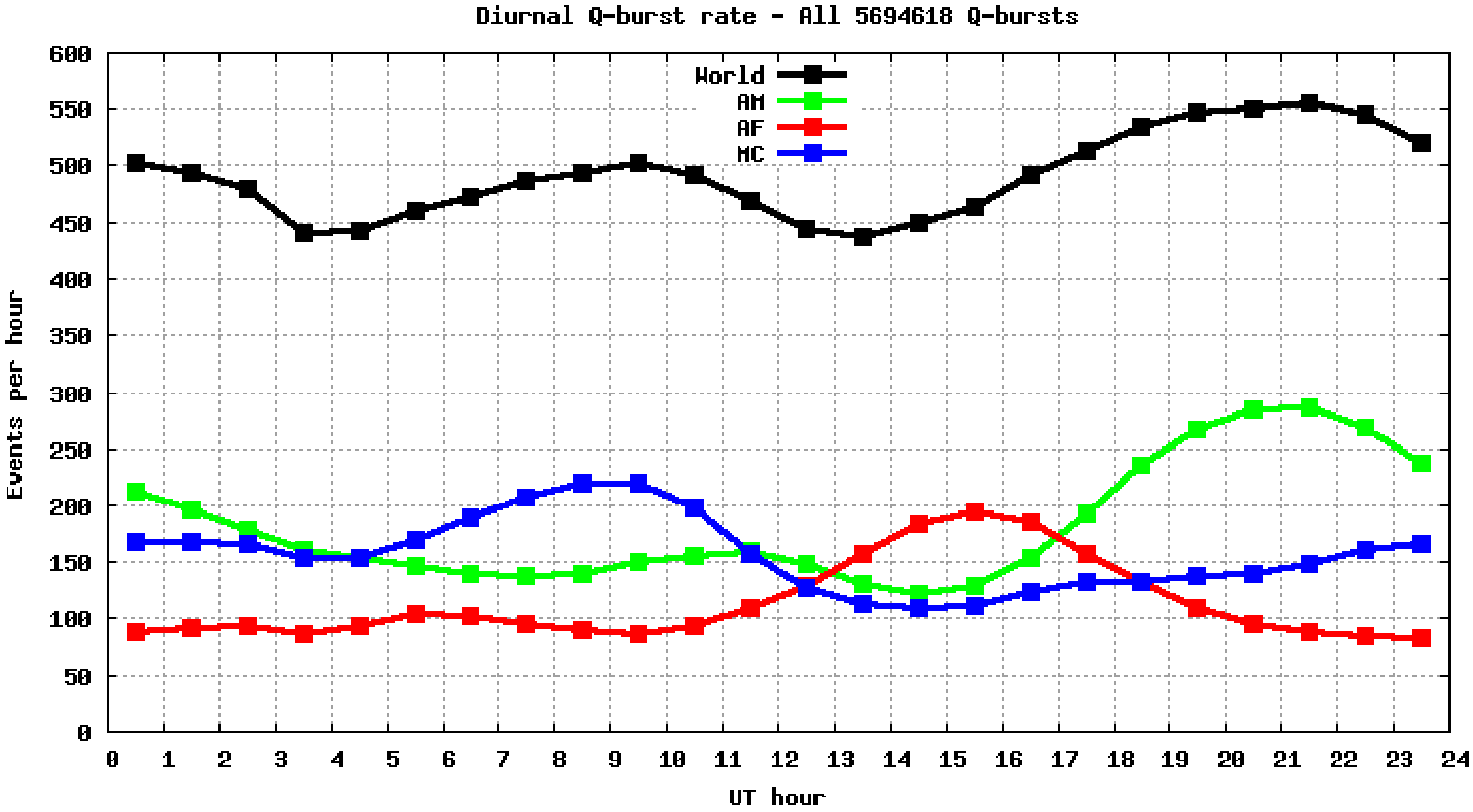

Latitude Dependence & Regional Polarity

- Analysis: Average event rate and total charge moment by latitude.
- Observation: Positive events dominate the total charge moment in the mid-latitudes, indicating stronger continuing currents.

Regional Polarity:

- Africa: ~47% positive.
- Maritime Continent: ~54% positive.
- Americas: ~43% positive.

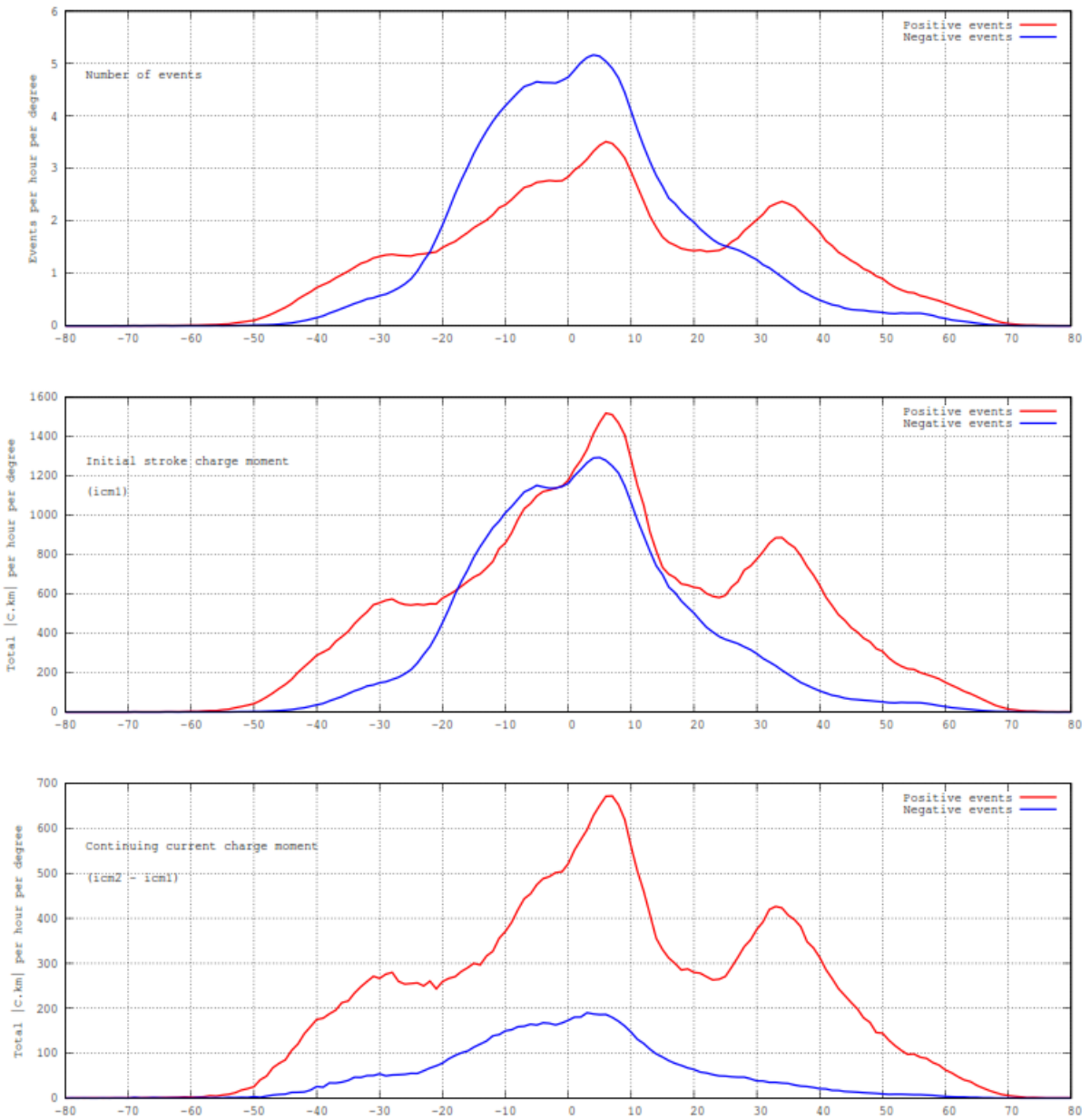

Charge Moment Density: Global Distribution

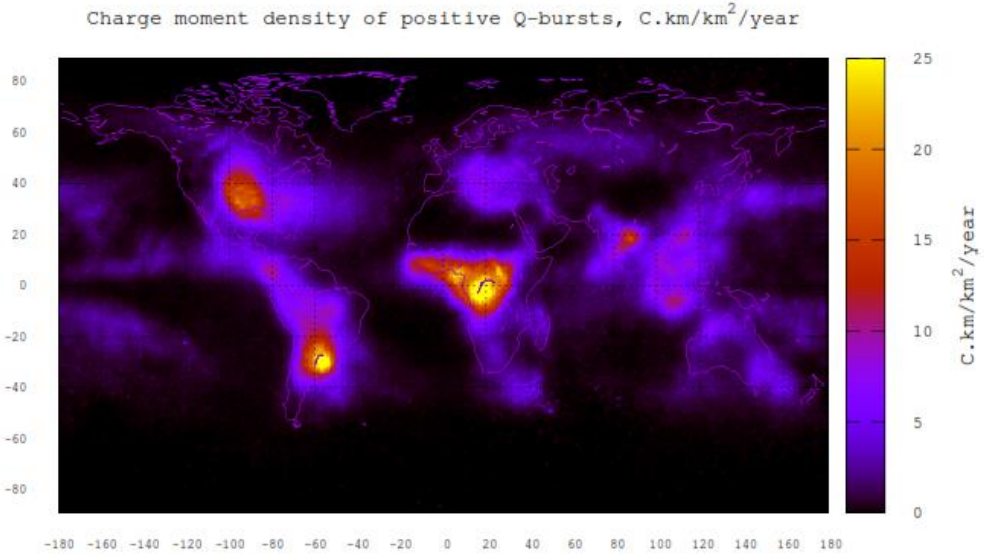

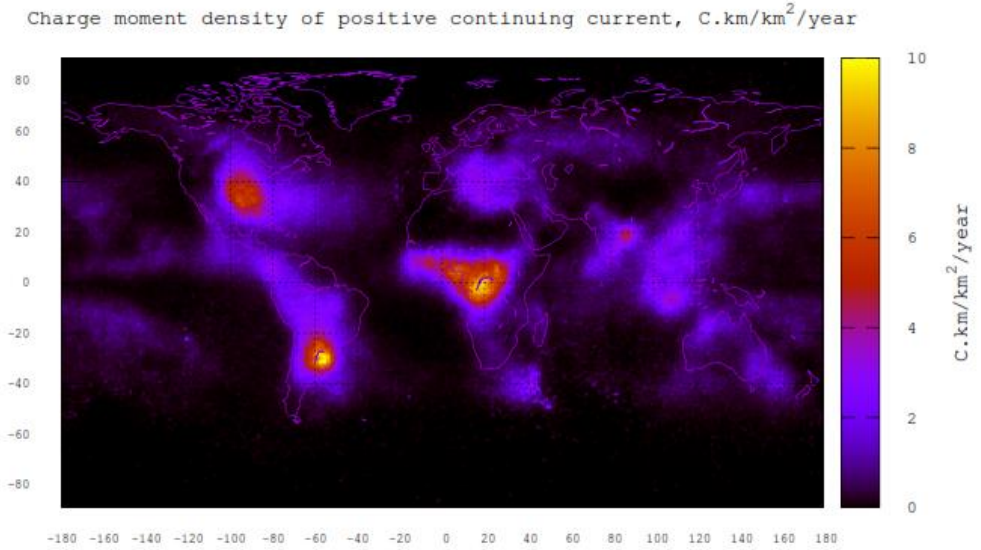

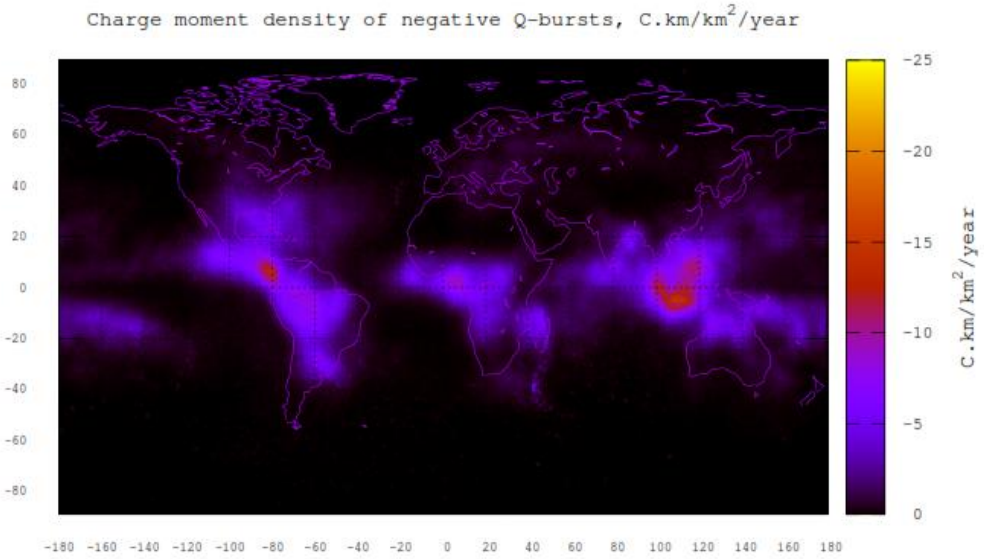

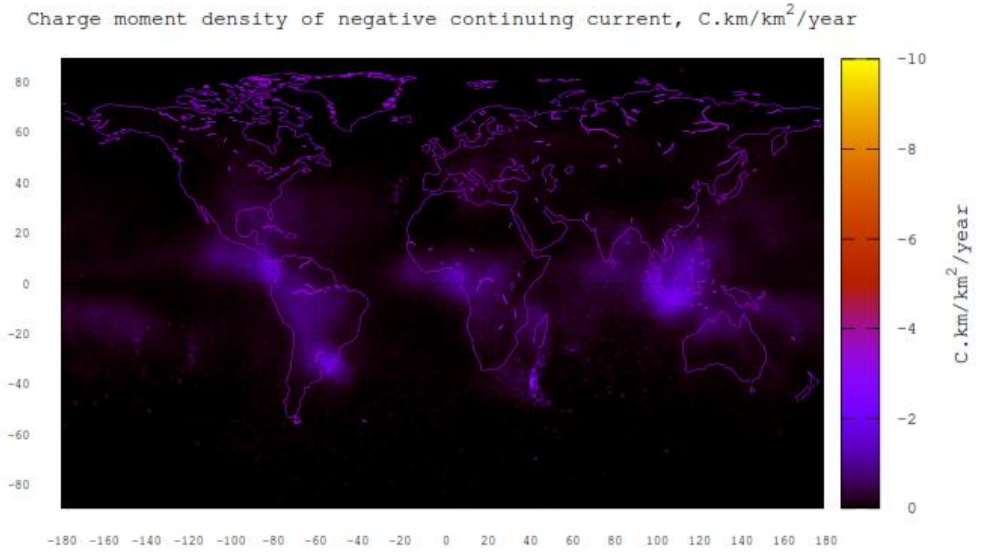

Temporal Dynamics: Diurnal Patterns

Analysis: Average hourly event rates across three main regions.

Pattern:

- Diurnal curves match the expected migration of thunderstorm activity across the globe, late afternoon peak.
- The local time morning peak is a puzzle and requires careful consideration of the propagation factors (role of day-night terminator)

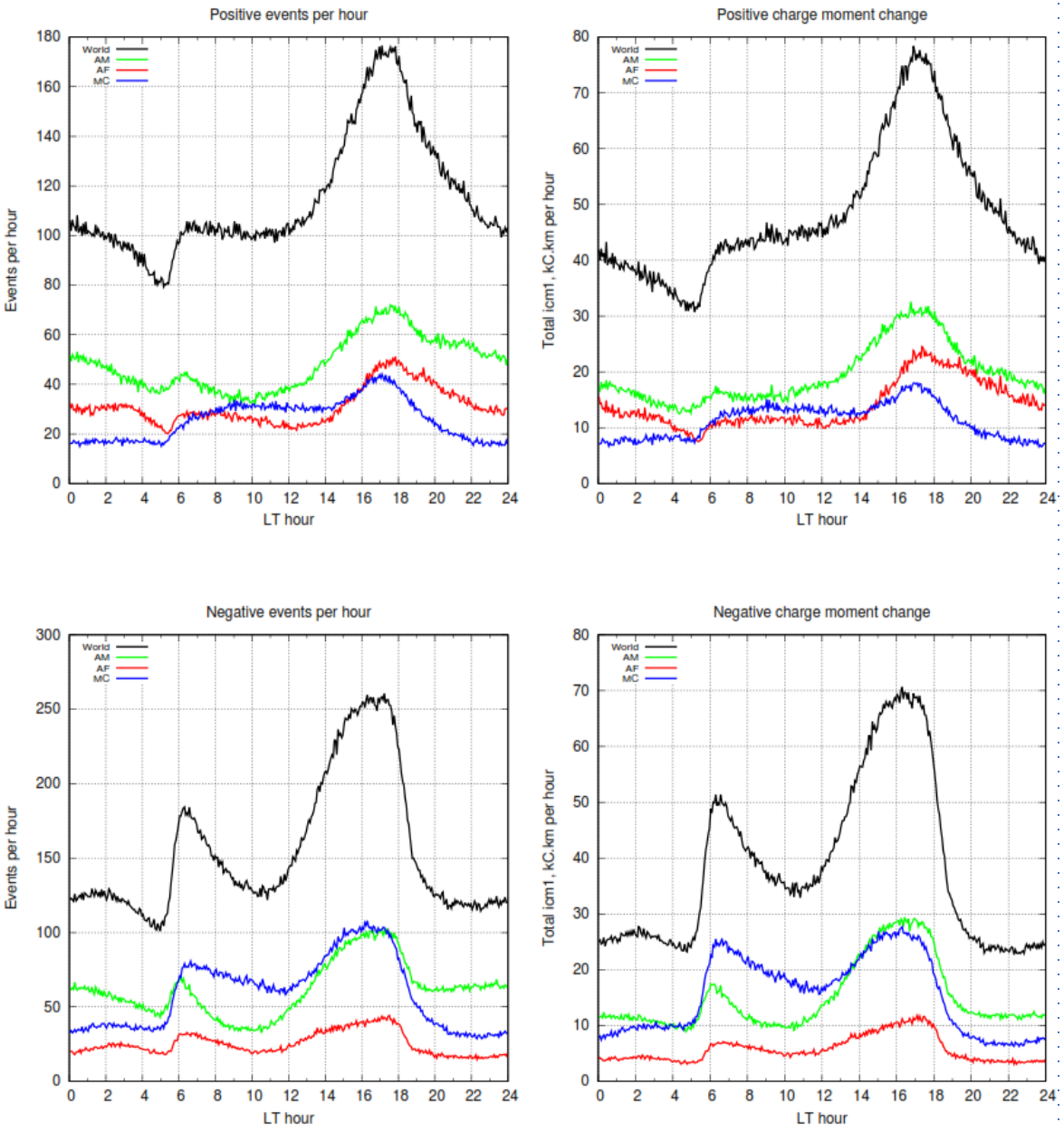

A Deeper Look: The Segmented Path Model

Limitation of 2D Model: Launch azimuth isn't representative of the whole path (especially long ones).

Advanced Approach:

- Divide each propagation path into ~500 km segments.
- Assume uniform conditions (illumination, magnetic field) per segment.
- Solve a large linear system to find the propagation delay per segment type.
- Yet to implement the segmented path model

B_h (nT)	-90/-60	-60/-40	-40/-20	-20/0	0/+20	+20/+40	+40/+60	+60/+90
-36000	0.941	0.915	0.904	0.870	0.778	0.789	0.782	0.797
-32000	0.909	0.905	0.897	0.872	0.800	0.802	0.808	0.810
-28000	0.899	0.904	0.900	0.870	0.794	0.789	0.790	0.800
-24000	0.908	0.913	0.899	0.856	0.794	0.786	0.785	0.804
-20000	0.896	0.893	0.896	0.850	0.790	0.773	0.782	0.794
-16000	0.899	0.900	0.893	0.834	0.779	0.760	0.771	0.803
-12000	0.880	0.895	0.890	0.831	0.773	0.771	0.775	0.786
-8000	0.894	0.885	0.880	0.838	0.775	0.766	0.782	0.800
-4000	0.884	0.878	0.875	0.839	0.773	0.765	0.774	0.792
0	0.879	0.868	0.866	0.833	0.777	0.764	0.772	0.800
+4000	0.898	0.886	0.876	0.846	0.782	0.758	0.774	0.796
+8000	0.918	0.901	0.897	0.842	0.791	0.771	0.776	0.800
+12000	0.898	0.891	0.882	0.837	0.787	0.771	0.772	0.790
+16000	0.899	0.893	0.885	0.840	0.782	0.775	0.780	0.797
+20000	0.928	0.927	0.918	0.877	0.797	0.796	0.801	0.804
+24000	0.881	0.894	0.913	0.864	0.781	0.783	0.805	0.801
+28000	0.911	0.910	0.912	0.864	0.792	0.773	0.792	0.807
+32000	0.941	0.923	0.927	0.875	0.805	0.800	0.795	0.806
+36000	0.970	0.954	0.960	0.900	0.824	0.815	0.823	0.836

Outcome: Created a detailed table of velocity factors based on local Sun elevation and transverse magnetic field.

Mysteries & Puzzles (Open Questions)

Unexplained Phenomena:

- Increased daytime velocity for Sun >60° elevation.
- A surge in negative Q-burst rates around 06:00 local time, not seen in ordinary strokes.
- Pre-event Quiescence: A period of 100-250 ms before a Q-burst where ordinary lightning is inhibited.
- Post-event Activity: A 5x spike in ordinary strokes following negative Q-bursts.

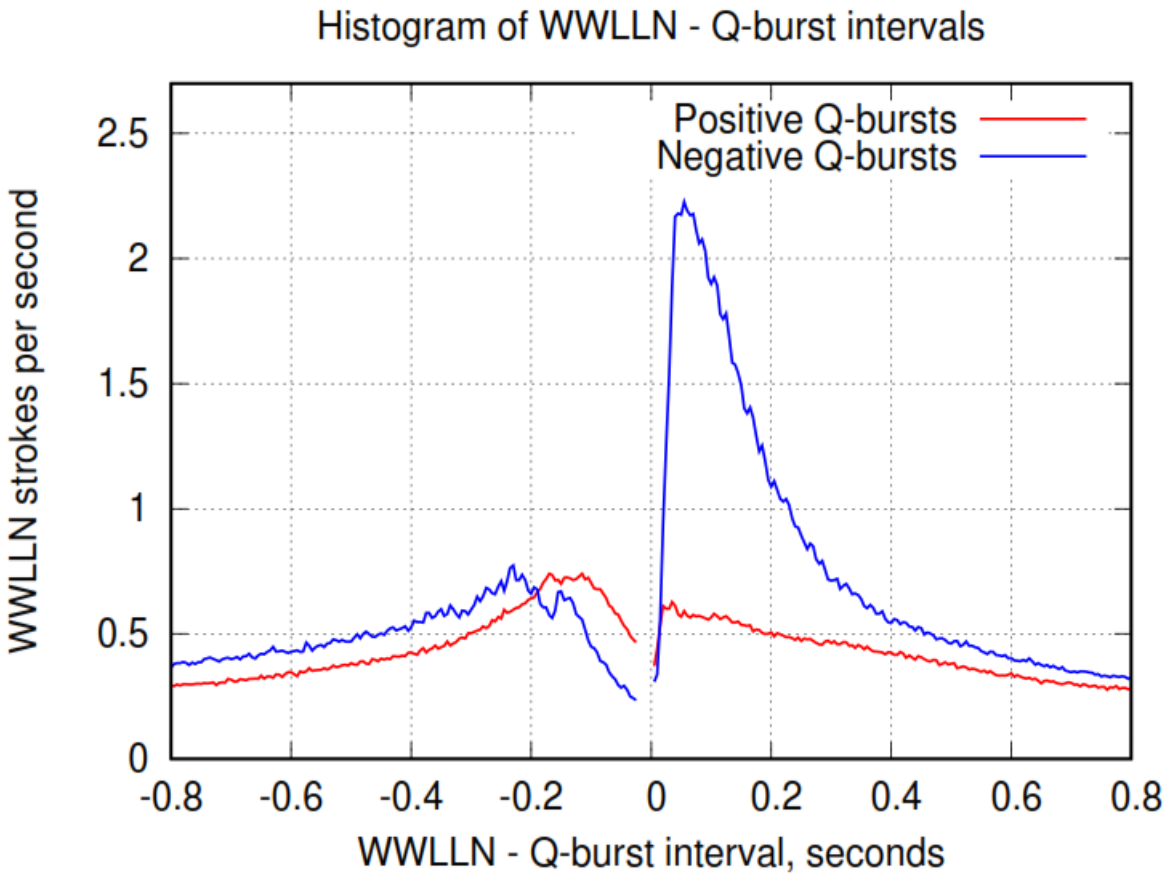

Key Findings & Conclusions

- Successfully located over 4.5 million Q-bursts using a network of six ELF magnetometers.
- Developed a 2D propagation model that improved location accuracy to 417 km.
- Provided global maps of Q-burst occurrence and charge moment, revealing distinct patterns for positive and negative strokes.
- Characterized the source current moment for millions of events.
- Identified new and intriguing temporal relationships between Q-bursts and ordinary lightning, pointing to complex storm dynamics.

Future Work & References

- Implement the segmented path model for final solution refinement.
- Use the massive dataset to further refine the empirical propagation model iteratively.
- Explore the physical mechanisms behind the "puzzles" (pre-event quiescence, etc.).

References:

- HeartMath Institute. "The Global Coherence Monitoring System“ [https://www.heartmath.org/gci/gcms/]
- Open source software package, vlfrx-tools (Simplified BSD License) [https://abelian.vvsindia.com/vlfrx-tools/vlfrx-tools.html
- Indian Lightning Detection Network (ILDN) [https://ildn.in]

Acknowledgments

- Sincere thanks to HeartMath Institute, WWLLN, all collaborators, and funding source (NSF) to support my visit to MIT in 2022 and 2024.
- A special thank to all the co-authors for their active support, especially Earle Williams. Without his constant inspiration and critical guidance, this work could not have been possible.
- Deepest and heartiest gratitude to Vadim C. Mushtak (posthumous) and Paul Nicholson (posthumous). **This work is dedicated to them and their beloved family.**

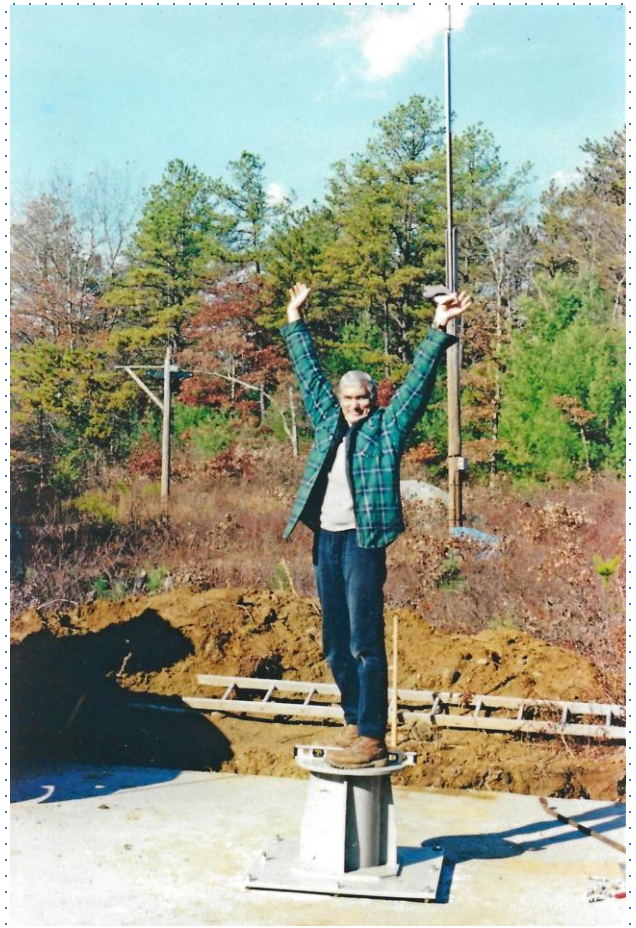

Vadim C. Mushtak (1947–2013)

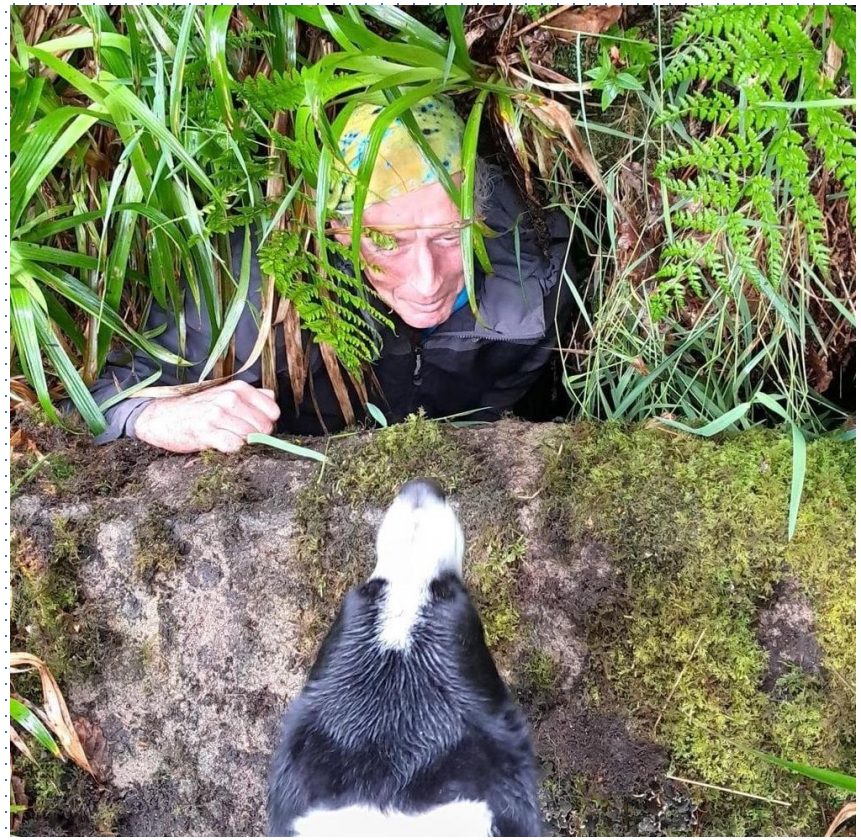

Paul Nicholson (1959–2025)

https://hamsci.org/hamsci2026

https://agupubs.onlinelibrary.wiley.com/doi/pdf/10.1002/2014EO200006

Thanks

Questions and Discussion